

Ion transfer and adsorption of water-soluble metal complexes of 8-hydroxyquinoline derivatives at the water|1,2-dichloroethane interface

メタデータ	言語: eng 出版者: 公開日: 2022-11-04 キーワード (Ja): キーワード (En): 作成者: メールアドレス: 所属:
URL	https://doi.org/10.24517/00067812

This work is licensed under a Creative Commons Attribution-NonCommercial-ShareAlike 3.0 International License.



Supplementary material

Ion transfer and adsorption of water-soluble metal
complexes of 8-hydroxyquinoline derivatives at
the water|1,2-dichloroethane Interface

Sho Yamamoto ^a, Shohei Kanai ^a, Marie Takeyama ^b, Yoshio Nishiyama ^c, Hisanori Imura ^c, and
Hirohisa Nagatani ^{c,*}

^aDivision of Material Chemistry, Graduate School of Natural Science and Technology,
Kanazawa University, Kakuma, Kanazawa 920-1192, Japan

^bSchool of Chemistry, College of Science and Engineering, Kanazawa University, Kakuma,
Kanazawa 920-1192, Japan

^cFaculty of Chemistry, Institute of Science and Engineering, Kanazawa University, Kakuma,
Kanazawa 920-1192, Japan

*To whom correspondence should be addressed: H. Nagatani

E-mail: nagatani@se.kanazawa-u.ac.jp

S1 Ionic partition diagram of QS species

The ionic partition diagram of QS in **Figure 2** was determined by analyzing the half-wave potential ($\Delta_o^w \phi_{1/2}$) obtained from the cyclic voltammograms (CVs) (**Figure S1**), considering acid-base equilibria in aqueous solution, ion transfer of the monoanionic HQS^- , and partition of neutral species (H_2QS) (**Figure S2**) [1, 2]. The cell composition was shown in **Figure 1 (Cell II)**. CVs were measured by using a four-electrode cylindrical cell with an interfacial area of 1.0 cm^2 .

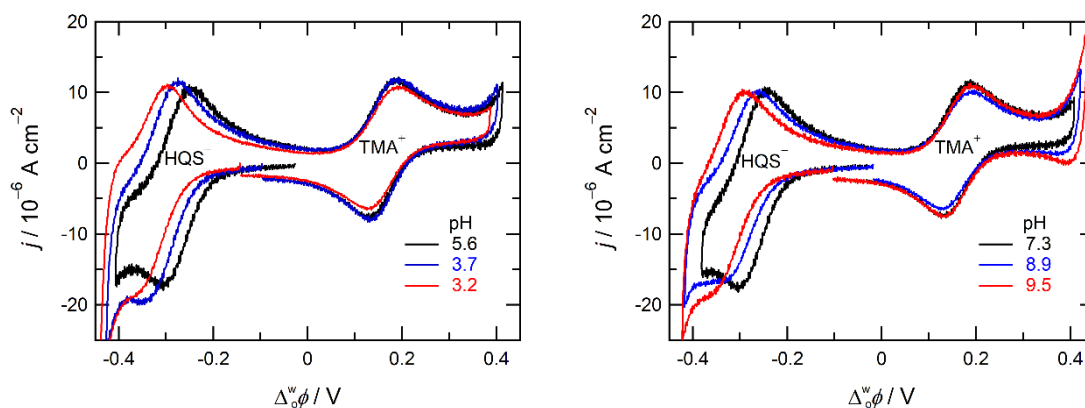


Figure S1. Typical CVs measured for QS species at various pHs in the presence of tetramethylammonium (TMA^+) as an internal reference.

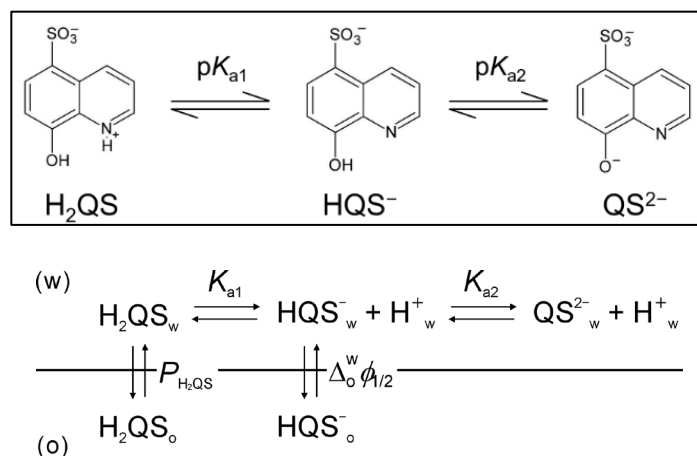


Figure S2. The reaction scheme for the partition of QS species associated with the acid-base equilibrium in the aqueous phase. The subscripts w and o denote the aqueous and organic species, respectively.

The peak separation of ~60 mV was indicative of the monovalent ion transfer across the water|DCE interface, i.e., HQS^- . In this case, the Nernst equation for the ion transfer of HQS^- is described as

$$\Delta_o^w \phi = \Delta_o^w \phi_{\text{HQS}^-}^{\circ} - \frac{2.303RT}{F} \log \frac{[\text{HQS}^-]_o}{[\text{HQS}^-]_w} \quad (\text{S-1-1})$$

where $\Delta_o^w \phi_{\text{HQS}^-}^{\circ}$ is the formal transfer potential. When the dissociation or protonation of HQS^- is negligible and the concentrations of HQS^- in both phases are equal to each other, eq. (S-1-1) is simplified to

$$\Delta_o^w \phi = \Delta_o^w \phi_{\text{HQS}^-}^{\circ} \quad (\text{S-1-2})$$

Then eq. (S-1-2) is the equiconcentration boundary line of HQS^-_w and HQS^-_o . $\Delta_o^w \phi_{\text{HQS}^-}^{\circ}$ was determined from $\Delta_o^w \phi_{1/2}$ at $5 < \text{pH} < 8$ as -0.277 ± 0.003 V. Considering that the distribution of the neutral H_2QS and acid-base equilibrium of QS species in acidic aqueous solutions, K_{a1} is expressed as a function of pH and the partition coefficient ($P_{\text{H}_2\text{QS}} = [\text{H}_2\text{QS}]_o / [\text{H}_2\text{QS}]_w$) under dilute conditions.

$$K_{a1} = \frac{[\text{HQS}^-]_w [\text{H}^+]_w}{[\text{H}_2\text{QS}]_w} = \frac{P_{\text{H}_2\text{QS}} [\text{HQS}^-]_w [\text{H}^+]_w}{[\text{H}_2\text{QS}]_o} \quad (\text{S-1-3})$$

$$\text{p}K_{a1} = -\log P_{\text{H}_2\text{QS}} - \log \frac{[\text{HQS}^-]_w}{[\text{H}_2\text{QS}]_o} + \text{pH} \quad (\text{S-1-4})$$

The equiconcentration boundary line of H_2QS and aqueous HQS^-_w is given by

$$\text{pH} = \text{p}K_{a1} + \log P_{\text{H}_2\text{QS}} \quad (\text{S-1-5})$$

The partition coefficient ($\log P_{\text{H}_2\text{QS}}$) of the neutral H_2QS was estimated as $\log P_{\text{H}_2\text{QS}} = 0.05$ by taking $\text{p}K_{a1} = 4.09$ [3]. Eq. (S-1-4) can also be rewritten as

$$\log \frac{[\text{HQS}^-]_o}{[\text{HQS}^-]_w} = \text{p}K_{a1} - \text{pH} + \log P_{\text{H}_2\text{QS}} + \log \frac{[\text{HQS}^-]_o}{[\text{H}_2\text{QS}]_o} \quad (\text{S-1-6})$$

From eqs. (S-1-1) and (S-1-6),

$$\Delta_o^w \phi = \Delta_o^w \phi_{\text{HQS}^-}^{\circ} + \frac{2.303RT}{F} \text{pH} - \frac{2.303RT}{F} \left(\text{p}K_{a1} + \log P_{\text{H}_2\text{QS}} + \log \frac{[\text{HQS}^-]_o}{[\text{H}_2\text{QS}]_o} \right) \quad (\text{S-1-7})$$

The boundary line between H_2QS_o and HQS^-_o is obtained as

$$\Delta_o^w \phi = \Delta_o^w \phi_{\text{HQS}^-}^{\circ} + \frac{2.303RT}{F} \text{pH} - \frac{2.303RT}{F} (\text{p}K_{\text{a}1} + \log P_{\text{H}_2\text{QS}}) \quad (\text{S-1-8})$$

In a similar manner, the boundary line between HQS^-_{w} and $\text{QS}^{2-}_{\text{w}}$ is derived from $\text{p}K_{\text{a}2}$ (= 8.66 [3]).

$$K_{\text{a}2} = \frac{[\text{QS}^{2-}]_{\text{w}}[\text{H}^+]_{\text{w}}}{[\text{HQS}^-]_{\text{w}}} = \frac{[\text{HQS}^-]_{\text{o}}}{[\text{HQS}^-]_{\text{w}}} \frac{[\text{QS}^{2-}]_{\text{w}}[\text{H}^+]_{\text{w}}}{[\text{HQS}^-]_{\text{o}}} \quad (\text{S-1-9})$$

$$\log \frac{[\text{HQS}^-]_{\text{o}}}{[\text{HQS}^-]_{\text{w}}} = \text{pH} - \text{p}K_{\text{a}2} - \log \frac{[\text{QS}^{2-}]_{\text{w}}}{[\text{HQS}^-]_{\text{o}}} \quad (\text{S-1-10})$$

From eqs. (S-1-1) and (S-1-10),

$$\Delta_o^w \phi = \Delta_o^w \phi_{\text{HQS}^-}^{\circ} - \frac{2.303RT}{F} \text{pH} + \frac{2.303RT}{F} \left(\text{p}K_{\text{a}2} + \log \frac{[\text{QS}^{2-}]_{\text{w}}}{[\text{HQS}^-]_{\text{o}}} \right) \quad (\text{S-1-11})$$

In the case of equiconcentration of $\text{QS}^{2-}_{\text{w}}$ and HQS^-_{o} , eq. (S-1-11) is reduced to

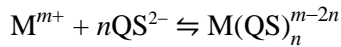
$$\Delta_o^w \phi = \Delta_o^w \phi_{\text{HQS}^-}^{\circ} - \frac{2.303RT}{F} \text{pH} + \frac{2.303RT}{F} \text{p}K_{\text{a}2} \quad (\text{S-1-12})$$

Finally, the boundary line of HQS^-_{w} and $\text{QS}^{2-}_{\text{w}}$ is written as the following simple form.

$$\text{pH} = \text{p}K_{\text{a}2} \quad (\text{S-1-13})$$

S2 Speciation analysis of QS in aqueous solutions

The stoichiometry for metal complex formation with QS varies from 1:1 to 1:3 (metal:ligand) depending on metal ions and pH conditions in the aqueous solution. The stability constants of metal complexes (β_n) in literature are listed in **Table S1** [4-6].



$$\beta_n = \frac{[\text{M}(\text{QS})_n^{m-2n}]}{[\text{M}^{m+}][\text{QS}^{2-}]^n} \quad (\text{S-2-1})$$

where $m = 1, 2, 3$ and $n = 1, 2$. Taking into account the formation of metal hydroxides, the total concentrations of metal ion (c_{M}) and ligand (c_{L}) are given by

$$c_{\text{M}} = [\text{M}] + [\text{ML}] + \cdots + [\text{ML}_n] + [\text{M}(\text{OH})] + [\text{M}(\text{OH})_2] + \cdots + [\text{M}(\text{OH})_m] \quad (\text{S-2-2})$$

$$c_L = [L] + [ML] + 2[ML_2] + 3[ML_3] \quad (\text{S-2-3})$$

where

$$[L] = [L] + [HL] + [H_2L] = [L] \left(1 + \frac{[H^+]}{K_{a2}} + \frac{[H^+]^2}{K_{a1}K_{a2}} \right) \quad (\text{S-2-4})$$

The speciation of Al(III), Zn(II) and Cu(II) complexes with QS were calculated as a function of pH from eqs. (S-2-1)–(S-2-4) and the stability constants of QS complexes (**Table S1**).

Table S1. Stability constants (β_n) of QS complexes

metal ion	$\log\beta_1$	$\log\beta_2$	$\log\beta_3$	Ref.
Al(III)	8.95	17.43	24.58	[4]
Zn(II)	7.54	14.32	–	[5]
Cu(II)	12.50	23.10	–	[6]

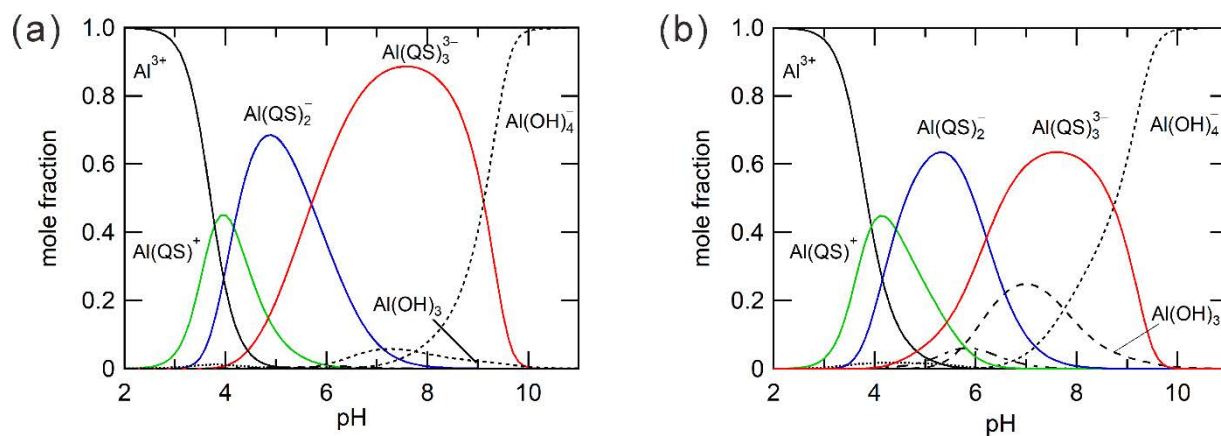


Figure S3. Speciation curves of Al(III)-QS complexes as a function of pH. The total concentrations of aluminum(III) ion and QS were taken as $[Al(III)] = 1.0 \times 10^{-4} \text{ mol dm}^{-3}$, $[QS] =$ (a) $3.0 \times 10^{-4} \text{ mol dm}^{-3}$ and (b) $2.0 \times 10^{-4} \text{ mol dm}^{-3}$, respectively

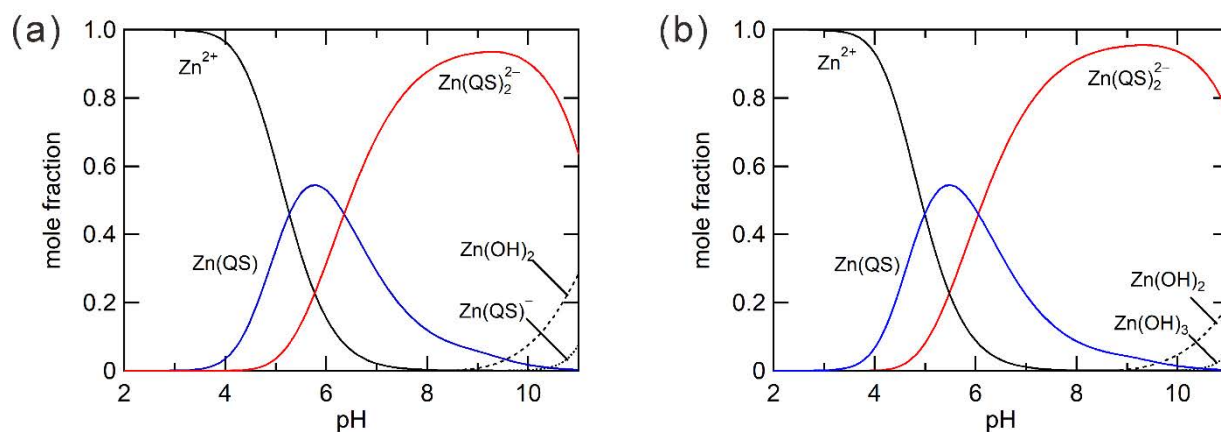


Figure S4. Speciation curves of Zn(II)-QS complexes as a function of pH. The concentrations of zinc(II) ion and QS were taken as (a) $[Zn(II)] = 5.0 \times 10^{-5} \text{ mol dm}^{-3}$ and $[QS] = 1.0 \times 10^{-4} \text{ mol dm}^{-3}$, and (b) $[Zn(II)] = 1.0 \times 10^{-4} \text{ mol dm}^{-3}$ and $[QS] = 2.0 \times 10^{-4} \text{ mol dm}^{-3}$, respectively.

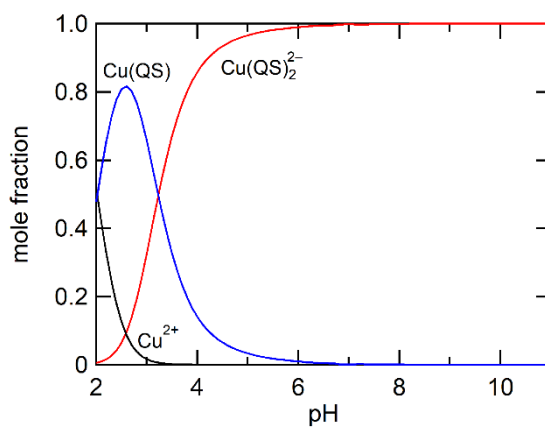


Figure S5. Speciation curves of Cu(II)-QS complexes as a function of pH. The concentrations of copper(II) ion and QS were taken as $[Cu(II)] = 1.0 \times 10^{-4} \text{ mol dm}^{-3}$ and $[QS] = 2.0 \times 10^{-4} \text{ mol dm}^{-3}$, respectively.

S3 Voltammetric responses of QS complexes at the water|DCE interface

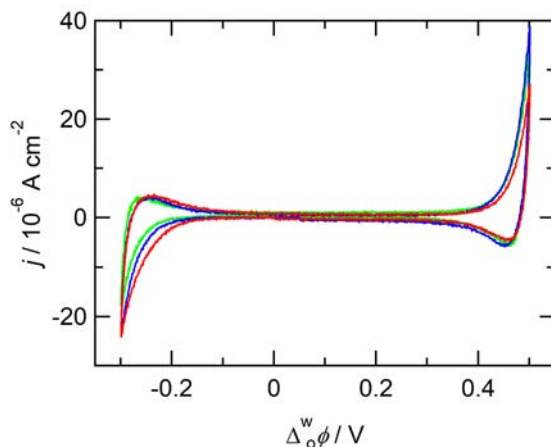


Figure S6. CVs measured for Al(III)-QS at pH 7.3 (red), Zn(II)-QS at pH 7.5 (blue), and Cu(II)-QS at pH 7.3 (green). The potential sweep rate was 20 mV s^{-1} . The concentrations were $[\text{Al(III)}] = 1.0 \times 10^{-4} \text{ mol dm}^{-3}$ and $[\text{QS}] = 3.0 \times 10^{-4} \text{ mol dm}^{-3}$, $[\text{Zn(II)}] = 1.0 \times 10^{-4} \text{ mol dm}^{-3}$ and $[\text{QS}] = 2.0 \times 10^{-4} \text{ mol dm}^{-3}$, $[\text{Cu(II)}] = 1.0 \times 10^{-4} \text{ mol dm}^{-3}$ and $[\text{QS}] = 2.0 \times 10^{-4} \text{ mol dm}^{-3}$, respectively.

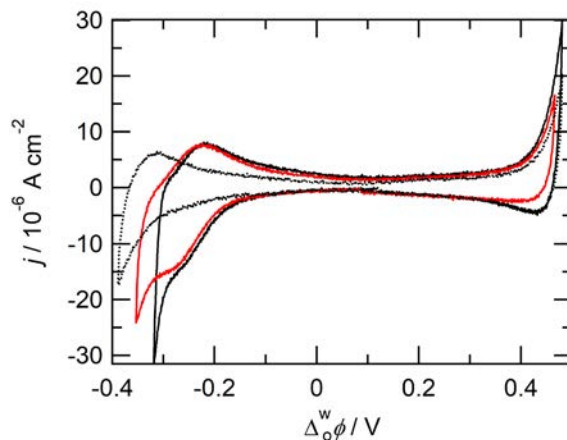


Figure S7. CVs measured in the Al(III)-QS system at pH 7.0 (black) and pH 4.9 (red). The dotted line depicts the base electrolyte system. The potential sweep rate was 50 mV s^{-1} . The concentrations were (pH 7.0) $[\text{Al(III)}] = 1.0 \times 10^{-4} \text{ mol dm}^{-3}$ and $[\text{QS}] = 3.0 \times 10^{-4} \text{ mol dm}^{-3}$, and (pH 4.9) $[\text{Al(III)}] = 1.0 \times 10^{-4} \text{ mol dm}^{-3}$ and $[\text{QS}] = 2.0 \times 10^{-4} \text{ mol dm}^{-3}$, respectively.

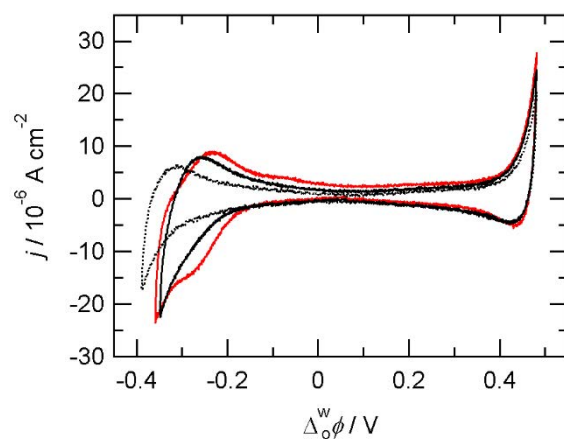


Figure S8. CVs measured in the Zn(II)-QS systems at pH 7.0 (black) and pH 6.1 (red). (a) The dotted line depicts the base electrolyte system. The potential sweep rate was (a) 50 mV s^{-1} . The concentrations were $[\text{Zn(II)}] = 5.0 \times 10^{-5} \text{ mol dm}^{-3}$ and $[\text{QS}] = 1.0 \times 10^{-4} \text{ mol dm}^{-3}$.

S4 Fluorescence spectra of QS complexes

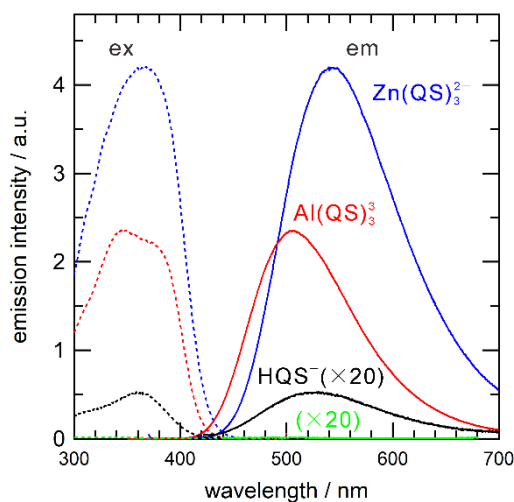


Figure S9. Excitation (dotted line) and emission (solid line) spectra of the QS complexes in aqueous solutions. The black, red, blue, and green lines depict HQS^- at pH 8.0, Al(QS)_3^{3-} at pH 7.3, Zn(QS)_2^{2-} at pH 7.5, and Cu(QS)_2^{2-} at pH 7.3, respectively. The spectra measured for HQS^- and Cu(QS)_2^{2-} were shown vertically expanded by a factor of 20 because of low emission intensities.

S5. PMF responses for $\text{Zn}(\text{QS})_2^{2-}$ measured in p- and s-polarized excitation modes

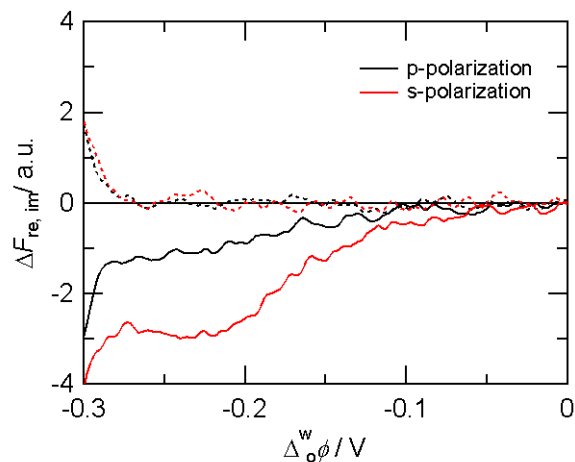


Figure S10. Potential dependences of the PMF responses for $\text{Zn}(\text{QS})_2^{2-}$ at pH 7.0. The black and red lines were measured by the s- and p-polarized excitation beams, respectively. The solid and dotted lines depict the real and imaginary components, respectively.

S6. PM-TIRF responses for Al(III)-QS and Zn(II)-QS complexes

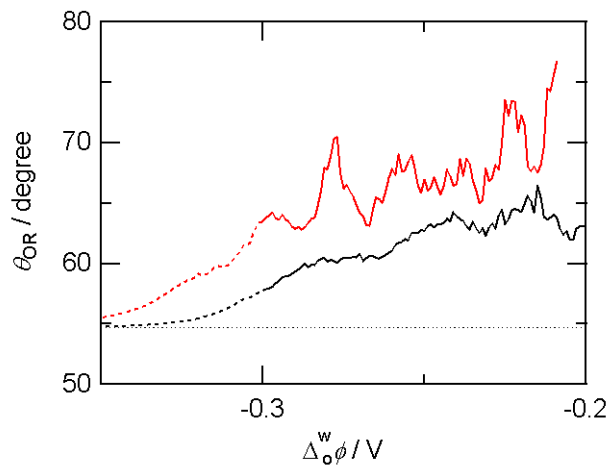


Figure S11. Potential dependences of θ_{OR} in the Al(III)-QS systems at pH 7.0 (black) and 4.9 (red).

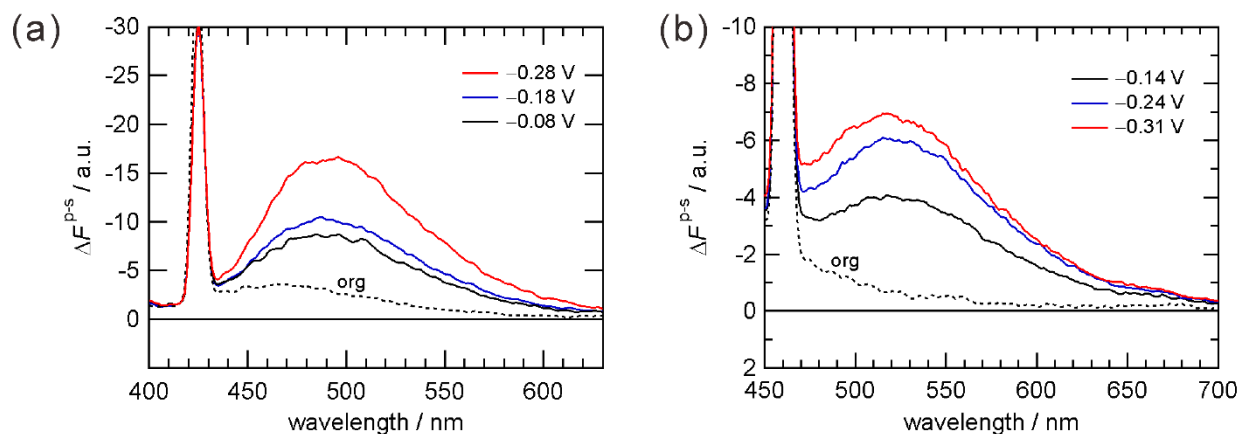


Figure S12. PM-TIRF spectra measured for (a) Al(III)-QS and (b) Zn(II)-QS at pH 7.0. The excitation wavelengths were (a) 376 nm and (b) 404 nm, respectively. The Raman bands around 424 nm or 460 nm superimposed on PM-TIRF spectra were subtracted by using the spectra originating from the bulk organic phase (dotted lines).

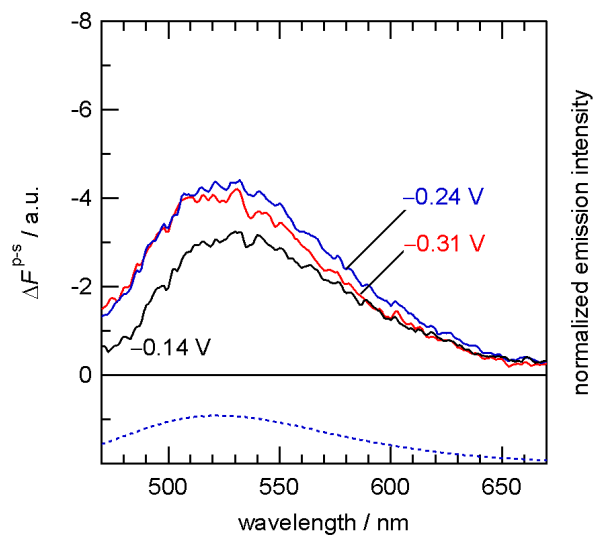


Figure S13. Potential dependence of PM-TIRF spectra in the Zn(II)-QS system at pH 6.1. The blue dashed line depicts the normalized fluorescence spectrum measured in aqueous solution.

S7. Capacitance curves and PMF responses for $\text{Zn}(\text{QC})_2^{2-}$ system

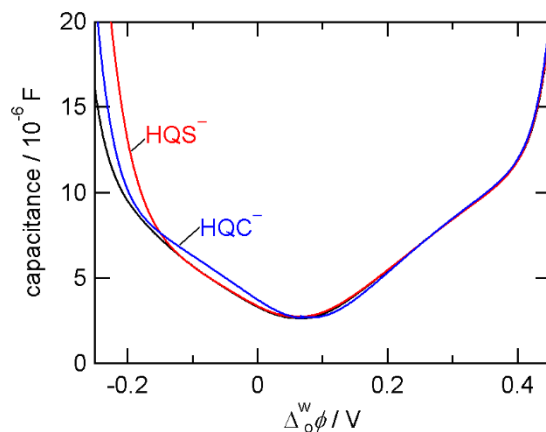


Figure S14. Capacitance curves measured for free HQS^- at pH 7.6 (red) and HQC^- at pH 8.1 (blue). The black line depicts the base electrolyte system. The concentration of QS and QC was $1.0 \times 10^{-4} \text{ mol dm}^{-3}$.

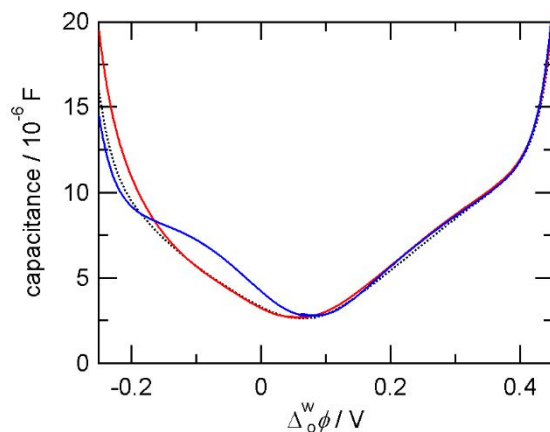


Figure S15. Capacitance curves measured for $\text{Zn}(\text{QS})_2^{2-}$ at pH 7.4 (red) and $\text{Zn}(\text{QC})_2^{2-}$ at pH 7.7 (blue). The black line depicts base electrolyte system. The concentrations were $[\text{Zn}(\text{II})] = 1.0 \times 10^{-4} \text{ mol dm}^{-3}$ and $[\text{QS}] = [\text{QC}] = 2.0 \times 10^{-4} \text{ mol dm}^{-3}$, respectively.

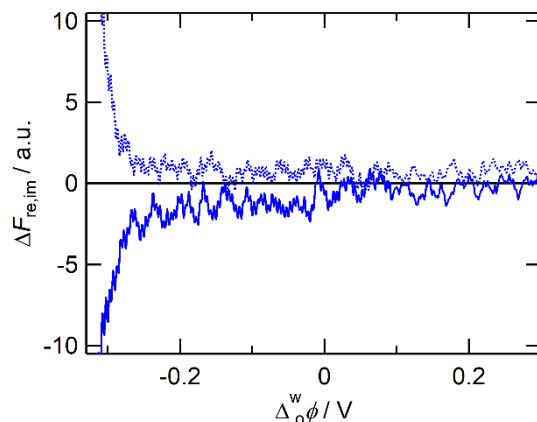


Figure S16. PMF responses measured for $\text{Zn}(\text{QC})_2^{2-}$ at pH 7.7. The solid and dotted lines depict the real and imaginary components, respectively. The potential modulation was 30 mV at 1 Hz with a sweep rate of 5 mV s^{-1} . The concentrations were $[\text{Zn}(\text{II})] = 1.0 \times 10^{-4} \text{ mol dm}^{-3}$ and $[\text{QC}] = 2.0 \times 10^{-4} \text{ mol dm}^{-3}$. The excitation and emission wavelengths were 376 nm and 492 nm, respectively.

References

- [1] V. Gobry, S. Ulmeanu, F. Reymond, G. Bouchard, P.-A. Carrupt, B. Testa, H.H. Girault, Generalization of Ionic Partition Diagrams to Lipophilic Compounds and to Biphasic Systems with Variable Phase Volume Ratios, *J. Am. Chem. Soc.* 123(43) (2001) 10684-10690.
- [2] F. Reymond, G. Steyaert, P.A. Carrupt, B. Testa, H. Girault, Ionic partition diagrams: A potential-pH representation, *J. Am. Chem. Soc.* 118(47) (1996) 11951-11957.
- [3] J. Fresco, H. Freiser, Stabilities of chelates of certain substituted 8-quinolinols, *Inorg. Chem.* 2(1) (1963) 82-85.
- [4] D. Badocco, A. Dean, V. Di Marco, P. Pastore, Electrochemical characterization of 8-hydroxyquinoline-5-sulphonate/aluminium(III) aqueous solutions, *Electrochim. Acta* 52(28) (2007) 7920-7926.
- [5] J.L. Beltrán, R. Codony, M.D. Prat, Evaluation of stability constants from multi-wavelength absorbance data: program STAR, *Anal. Chim. Acta* 276(2) (1993) 441-454.
- [6] V. Pacáková, P. Coufal, K. Štulík, Capillary electrophoresis of inorganic cations, *J. Chromatogr. A* 834(1) (1999) 257-275.